Biochemical and Biophysical Research Communications 452 (2014) 951–957

Contents lists available at ScienceDirect

Biochemical and Biophysical Research Communications

journal homepage: www.elsevier.com/locate/ybbrc

miR-135a inhibition protects A549 cells from LPS-induced apoptosis by targeting Bcl-2

Jing Zhao [a,1], Xu Li [a,1], Ming Zou [a], Jing He [a], Yingmin Han [a], Dianbin Wu [a], Huafeng Yang [a], Jianlin Wu [b,*]

[a] Department of Pharmacy, Affiliated Zhongshan Hospital of Dalian University, Dalian, China
[b] Department of Radiology, Affiliated Zhongshan Hospital of Dalian University, Dalian, China

ARTICLE INFO

Article history:
Received 28 August 2014
Available online 16 September 2014

Keywords:
MicroRNA-135a
Bcl-2
Apoptosis
Lipopolysaccharide

ABSTRACT

Acute lung injury (ALI) is a severe clinical condition with high morbidity and mortality. Apoptosis is a key pathologic feature of ALI, and Bcl-2 plays an important role during the pathogenesis of ALI via the regulation of apoptosis. However, the regulation of Bcl-2 during ALI, particularly through microRNAs, remains unclear. We hypothesize that certain miRNAs may play deleterious or protective roles in ALI via the regulation of Bcl-2. The LPS stimulation of A549 cells was used to mimic ALI in vitro. First, we confirmed that Bcl-2 is involved in LPS-induced apoptosis in A549 cells. Then, bioinformatic analyses and quantitative real-time polymerase chain reaction assays were performed to screen for miRNAs targeting Bcl-2. We observed that miR-135a was markedly increased in LPS-challenged A549 cells. miR-135a inhibition markedly restored Bcl-2 expression and protected A549 cells from LPS-induced apoptosis. Furthermore, bioinformatic analysis and luciferase activity assays were conducted to confirm that miR-135a binds directly to the 3′-untranslated region of Bcl-2 and suppresses its expression. Interestingly, the inhibition of miR-135a did not attenuate apoptosis under LPS-treated conditions when Bcl-2 was knocked down. Therefore, we suggest that miR-135a regulation of LPS-induced apoptosis in A549 cells may depend in part on the regulation of Bcl-2. The miR-135a/Bcl-2 signaling pathway may be a novel therapeutic target for the prevention of ALI.

1. Introduction

Acute lung injury (ALI) is a severe respiratory disorder with high morbidity and mortality [1]. The most common cause of ALI is sepsis resulting from bacterial infection, and such injury may damage pulmonary structure and function, eventually resulting in acute respiratory distress syndrome (ARDS) [2,3]. Lipopolysaccharide (LPS), which is located in the outer membrane of the cell walls of gram-negative bacteria, is a common trigger of sepsis [4]. Indeed, it is believed that LPS plays a critical role in mediating acute damage to respiratory epithelia during sepsis [5]. Previous studies have indicated that multiple signaling pathways are involved in this pathogenesis, and apoptosis has been demonstrated to play an important role during injury progression [6,7]. However, the specific mechanism of apoptosis within this context is extremely complicated and remains unclear.

Apoptosis is a type of programmed cell death and is highly modulated by both intrinsic and extrinsic apoptotic factors. The extrinsic pathway is activated through transmembrane death receptors, including Fas/CD95, tumor necrosis factor (TNF) and TNF-related apoptosis-inducing ligand, whereas the intrinsic pathway is mainly regulated by the Bcl-2 superfamily, including Bax, Bak and Bcl-2. Bcl-2 is a key intrinsic regulator of the apoptotic cascade, and it can block apoptosis by preventing mitochondrial permeabilization [8]. Previous studies have demonstrated that the selective inhibition of Bcl-2 promotes apoptosis during various pro-apoptotic attacks [9,10]. Furthermore, accumulating evidence from both in vivo and in vitro studies has demonstrated that Bcl-2 plays important roles in the development of ALI [11,12]. However, the detailed mechanism by which Bcl-2 is regulated during disease progression requires further investigation.

MicroRNAs (miRNAs) are small (~21 nucleotides long) endogenous RNA molecules that have been identified as important transcriptional and post-transcriptional regulators of gene expression. miRNAs inhibit gene expression mainly by binding to the 3′-untranslated regions (UTRs) of their target transcripts, causing translational cleavage or suppression of the mRNA. It has been firmly established that miRNAs regulate many key biological processes, including cell proliferation, differentiation, metabolism and especially apoptosis [13]. An increasing number of reports

* Corresponding author.
E-mail address: jianlinwu_du@163.com (J. Wu).
[1] The first two authors contributed equally to the work.

http://dx.doi.org/10.1016/j.bbrc.2014.09.025
0006-291X/

confirm that miRNAs can function as either pro-apoptotic or anti-apoptotic factors [14,15]. However, considering the critical role of Bcl-2 during the development of ALI, whether a miRNA might regulate Bcl-2 and thereby affect disease progression remains obscure.

Combined with previous studies [11,12], we demonstrate that Bcl-2 is strongly associated with an in vitro septic ALI model (LPS-induced injury in A549 cells). Based on the hypothesis that the LPS-induced alteration in Bcl-2 may be regulated by miRNAs, we used bioinformatic analyses to identify miRNAs that may bind to the 3′-UTR of Bcl-2 mRNA and then quantified their expression levels before and after LPS stimulation. We propose that some miRNAs may exert deleterious or protective effects and that these effects may depend on miRNA-mediated Bcl-2 alterations. Our results provide a novel therapeutic target in the management of sepsis-induced ALI.

2. Materials and methods

2.1. Cell culture and treatments

The human pulmonary epithelial cell line A549 was maintained in RPMI-1640 medium (Gibco, Carlsbad, CA, USA) supplemented with 10% fetal bovine serum (Gibco) and 1% glutamine and cultured at 37 °C in a humidified atmosphere of 5% CO_2. The cells were seeded in six-well plates at 80% confluence. Cells were treated with 1 μg/ml LPS (Sigma–Aldrich, St. Louis, MO, USA) or vehicle (dimethyl sulfoxide; Sigma–Aldrich) for 24 h, in accordance with a previously published method [16]. To avoid toxicity, the concentration of dimethyl sulfoxide in the medium never exceeded 0.1%.

2.2. Cell viability assay

Cell viability was quantitatively assessed with Cell Counting Kit-8 (Dojindo, Tokyo, Japan). Briefly, the viability assay was conducted in 96-well plates, and absorbance was assessed using a microplate reader at 450 nm according to the manufacturer's instructions.

2.3. In situ apoptosis staining

Apoptosis in vitro was measured by terminal deoxynucleotidyl transferase-mediated dUTP nick end-labeling (TUNEL) staining, which was performed as instructed using a commercially available kit (Roche Diagnostics, Mannheim, Germany). For nuclear counterstaining, 4′,6-diamidino-2-phenylindole (DAPI; Sigma–Aldrich) solution was used according to the manufacturer's recommendations. The apoptosis rate was determined as TUNEL-positive cells/DAPI.

2.4. Caspase-3 activity assay

Caspase-3 activity was determined using a commercial assay kit (Beyotime Institute of Biotechnology, Jiangsu, China) according to the manufacturer's instructions.

2.5. Western blot

Equal amounts of cellular protein extracts (40 μg) were separated by 15% sodium dodecyl sulfate polyacrylamide gel electrophoresis (Bio-Rad, Hercules, CA, USA) and transferred to polyvinylidene difluoride membranes (Millipore, Bedford, MA, USA). Each membrane was incubated overnight at 4 °C with a primary antibody against Bcl-2 or β-actin (Abcam, Cambridge, UK) and subsequently incubated with appropriate secondary antibodies at room temperature for 2 h. The membranes were exposed to enhanced chemiluminescence plus reagents (Thermo Fisher Scientific, Dartford, UK). Protein quantification was performed with a Biospectrum-510 imaging system (UVP, Upland, CA, USA).

2.6. Quantitative real-time polymerase chain reaction (PCR)

Total RNA, including miRNA, was extracted using a mirVana miRNA isolation kit (Ambion, Carlsbad, CA, USA). miR-135a was reverse transcribed using a specific stem-loop primer (Applied Biosystems, Carlsbad, CA, USA) and quantified by real-time PCR with the TaqMan MicroRNA assay kit (Applied Biosystems). U6 was used for the normalization of miR-135a expression. Bcl-2 mRNA expression was quantified by real-time PCR with a TaKaRa RNA PCR Kit (TaKaRa, Dalian, China) using primers synthesized by TaKaRa.

2.7. Bioinformatic analysis

Human Bcl-2 3′-UTR sequences were retrieved from the Entrez Nucleotide database (www.ncbi.nlm.nih.gov/nuccore). The potential miRNA binding site in the Bcl-2 3′-UTR was predicted by TargetScan (www.targetscan.org) and miRanda (www.micorrna.org).

2.8. Transfection of miRNA

Cells were seeded in 6-well plates and transfected at 70–80% confluence with a miR-135a mimic, miR-135a inhibitor or the negative control using Lipofectamine 2000 (Invitrogen, Carlsbad, CA, USA) according to the manufacturer's instructions. The mimic, inhibitor and corresponding negative control were all obtained from Genepharma (Shanghai, China).

2.9. Luciferase reporter assay for Bcl-2-3′-UTR targeting

Luciferase vectors including the 3′-UTR of Bcl-2 containing the Bcl-2-miR-135a response elements and the mutant were purchased from Genepharma. For the luciferase reporter experiment, A549 cells were seeded in 12-well plates and cotransfected with the luciferase reporter vectors and the miR-135a mimic, inhibitor or corresponding negative control. Luciferase activity was measured using the Dual-Light Chemiluminescent Reporter Gene Assay System (Applied Biosystems) and normalized to the β-galactosidase activity.

2.10. Lentiviral transduction of cells

A549 cells were transduced with a lentiviral-based Bcl-2 short hairpin RNA (shRNA; Genepharma) according to the manufacturer's instructions. Bcl-2 knockdown was confirmed by Western blotting.

2.11. Statistical analysis

All data are expressed as the mean ± standard deviation (SD). The statistical analysis was carried out using the SPSS 16.0 statistical software package (SPSS Inc., Chicago, IL, USA). Statistical comparisons between pairs of groups were analyzed by a two-tailed Student *t*-test. Statistical comparisons between multiple groups were analyzed with the Kruskal–Wallis test followed by the Wilcoxon Rank Sum test with Bonferroni adjustments (for non-normal distributions) or a one-way analysis of variance followed by the Student–Newman–Keuls test (for normal distributions). A *p*-value less than 0.05 was considered statistically significant.

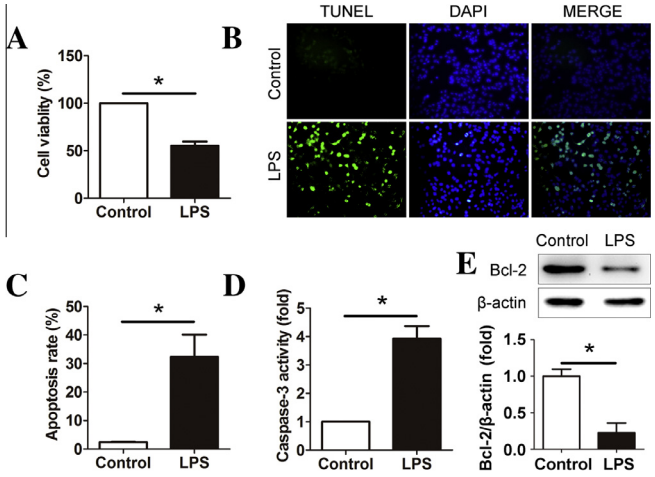

Fig. 1. Bcl-2 is involved in LPS-induced apoptosis in A549 cells. (A) A549 cell viability ($n = 6$). (B) Apoptosis observed by the TUNEL assay in A549 cells. The fluorescent signals from fragmented DNA (green) and nuclei (blue) were visualized and photographed under an inverted fluorescence microscope (200×). (C) The bar graph represents the quantification of TUNEL-positive cells; positive cells were counted in 10 visual fields. The apoptosis rate was determined as TUNEL-positive cells/DAPI. (D) Caspase-3 activity in A549 cells ($n = 6$). (E) Protein expression of Bcl-2. β-Actin was used as the internal control ($n = 3$). All data are expressed as the mean ± SD. $^*P < 0.05$. (For interpretation of the references to color in this figure legend, the reader is referred to the web version of this article.)

3. Results

3.1. Bcl-2 is involved in LPS-induced apoptosis in A549 cells

LPS is one of the major factors inducing ALI and is well known as an important mediator of apoptosis [5–7]. Due to the limitations of primary cell culture, LPS stimulation of A549 cells has been widely used to mimic ALI in vivo [14,16]. As shown in Fig. 1A, cell viability was significantly decreased after LPS treatment in comparison with the control group. To determine the apoptotic state

Table 1
Aberrant expression of Bcl-2 targeting miRNAs in LPS-induced apoptosis in A549 cells.

	MicroRNA	Fold of control	*P* value
Up-regulation	miR-15a	2.23	0.0016
	miR-15b	3.45	0.0005
	miR-135a	5.01	0.0007
	miR-195	1.82	0.0011
	miR-203	4.26	0.0005
Down-regulation	miR-497	0.68	0.0428
	miR-23a	0.85	0.0464
	miR-205	0.74	0.0251
	miR-199	0.72	0.0010

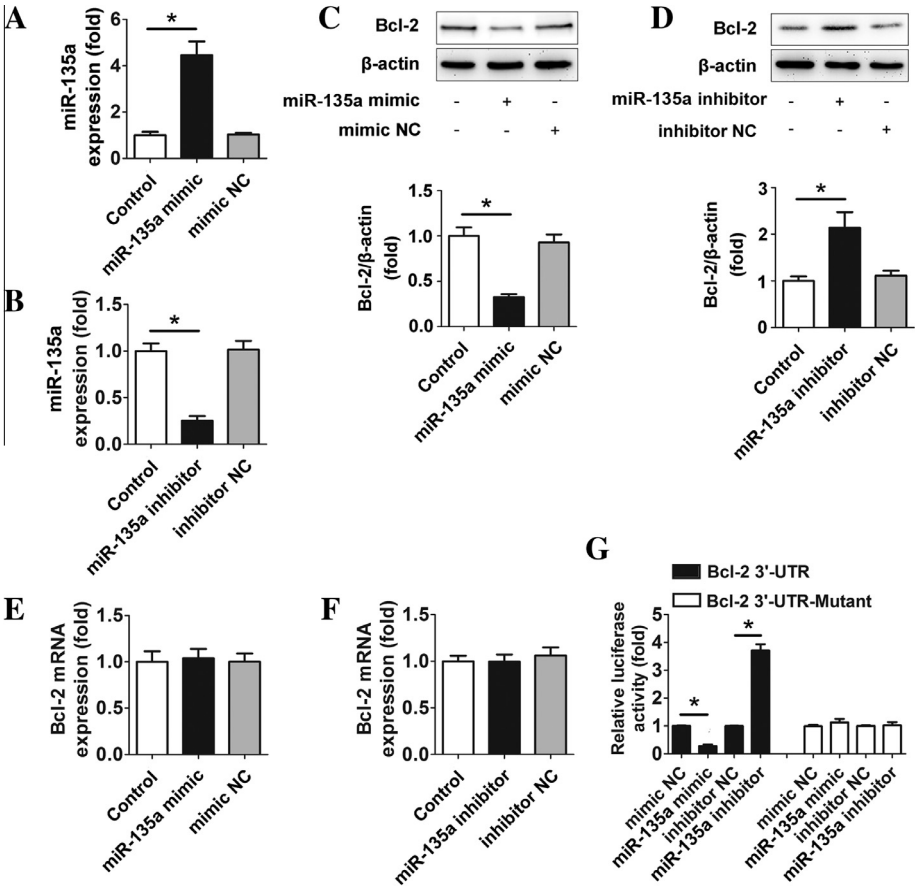

Fig. 2. miR-135a directly binds and downregulates Bcl-2. (A and B) The expression of miR-135a after treatment with miR-135a mimic or miR-135a inhibitor ($n = 6$). (C and D) Protein expression of Bcl-2 after treatment with miR-135a mimic or miR-135a inhibitor. β-Actin was used as the internal control ($n = 3$). (E and F) mRNA expression of Bcl-2 after treatment with miR-135a mimic or miR-135a inhibitor ($n = 6$). (G) A549 cells were transfected with wild-type or mutant 3′-UTR luciferase constructs and with miR-135a mimic, mimic NC, miR-135a inhibitor or inhibitor NC, as indicated ($n = 6$). All data are expressed as the mean ± SD. $^*P < 0.05$.

after LPS treatment, TUNEL staining was performed. As shown in Fig. 1B and C, the proportion of TUNEL-positive nuclei subjected to LPS treatment was significantly elevated when compared to the control group; this apoptosis was further confirmed by the caspase-3 activity assay (Fig. 1D). Moreover, a Western blot analysis was performed to determine whether the observed apoptosis involved Bcl-2 expression. As shown in Fig. 1E, after LPS treatment, the protein expression of Bcl-2 was significantly decreased compared with the control group. Combined with previous studies [11,12], we confirmed that Bcl-2 is involved in LPS-induced apoptosis in A549 cells.

3.2. miR-135a is upregulated among miRNAs targeting Bcl-2 after LPS treatment

To determine the potential involvement of Bcl-2-targeting miRNAs in LPS-induced apoptosis, we used bioinformatic analyses to search for miRNAs that can bind to the 3′-UTR of Bcl-2 and then quantified these potential binding miRNAs using real-time PCR. As shown in Table 1, compared to the control group, 5 miRNAs were upregulated, and 4 miRNAs were downregulated. The expression levels of other miRNAs targeting Bcl-2 (including miR-23a, miR-23b, miR-384 and miR-181a) were unchanged (data not shown). Among the miRNAs with expression levels that changed significantly during LPS-induced apoptosis, miR-135a was the most dramatically increased, by 5.01-fold.

3.3. miR-135a directly binds and downregulates Bcl-2

To determine whether miR-135a can regulate Bcl-2 expression, we transfected miR-135a mimic or inhibitor into A549 cells. Along with significant changes in the expression level of miR-135a (Fig. 2A and B), the protein expression of Bcl-2 was significantly decreased after miR-135a mimic transfection and increased after miR-135a inhibitor transfection (Fig. 2C and D). However, no apparent change in the Bcl-2 mRNA level was observed in either group (Fig. 2E and F).

To further validate whether a miR-135a binding site in the Bcl-2 3′-UTR mediated this repression, we inserted the Bcl-2 3′-UTR transcript or a mutated version into a luciferase system. Transfection of the miR-135a mimic clearly suppressed the luciferase activities of the 3′-UTR segment of Bcl-2, but the construct containing a mutant binding site abolished the inhibitory effect of the miR-135a mimic. In parallel, transfection of the miR-135a inhibitor increased the luciferase activity, whereas the mutant Bcl-2 3′-UTR abolished the positive effect of the miR-135a inhibitor (Fig. 2G).

3.4. miR-135a regulates LPS-induced apoptosis via Bcl-2 modulation

To confirm the role of miR-135a in LPS-induced apoptosis in A549 cells, we inhibited miR-135a expression in A549 cells exposed to LPS. As shown in Fig. 3A–D, the inhibition of miR-135a significantly increased cell viability and decreased

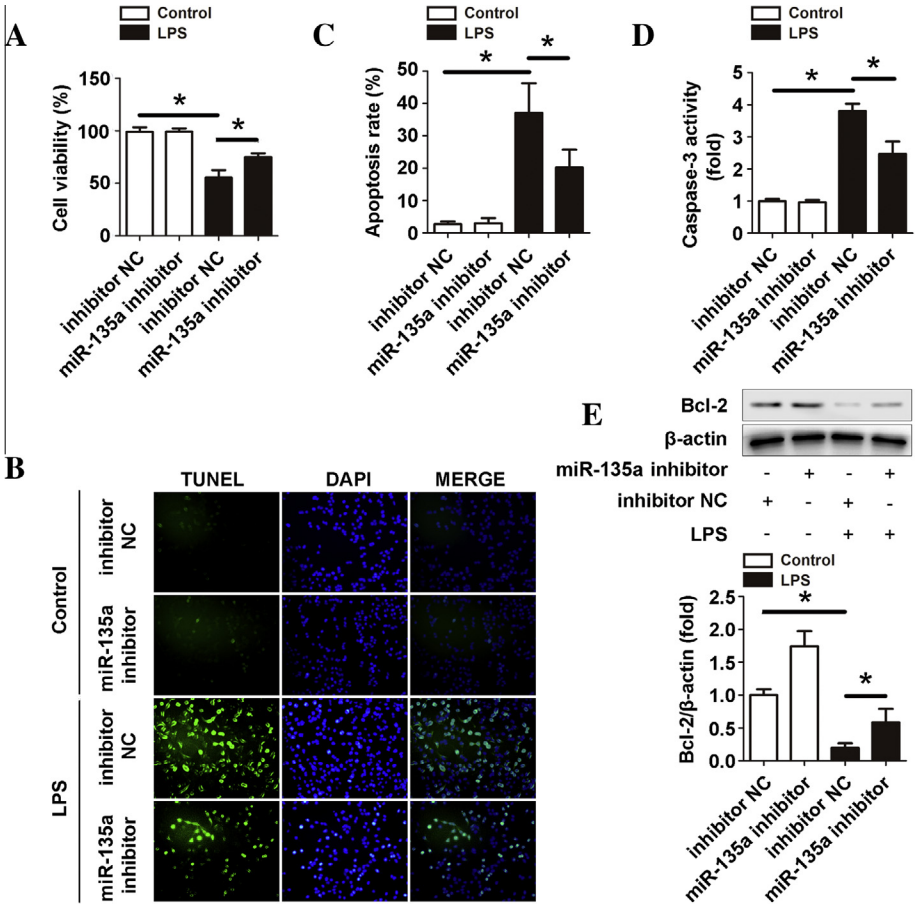

Fig. 3. miR-135a inhibition attenuates LPS-induced apoptosis in A549 cells. (A) A549 cell viability ($n = 6$). (B) Apoptosis observed by the TUNEL assay in A549 cells. The fluorescent signals from fragmented DNA (green) and nuclei (blue) were visualized and photographed under an inverted fluorescence microscope (200×). (C) The bar graph represents the quantification of TUNEL-positive cells; positive cells were counted in 10 visual fields. The apoptosis rate was determined as TUNEL-positive cells/DAPI. (D) Caspase-3 activity of A549 cells ($n = 6$). (E) Protein expression of Bcl-2. β-Actin was used as the internal control ($n = 3$). All data are expressed as the mean ± SD. $^*P < 0.05$. (For interpretation of the references to color in this figure legend, the reader is referred to the web version of this article.)

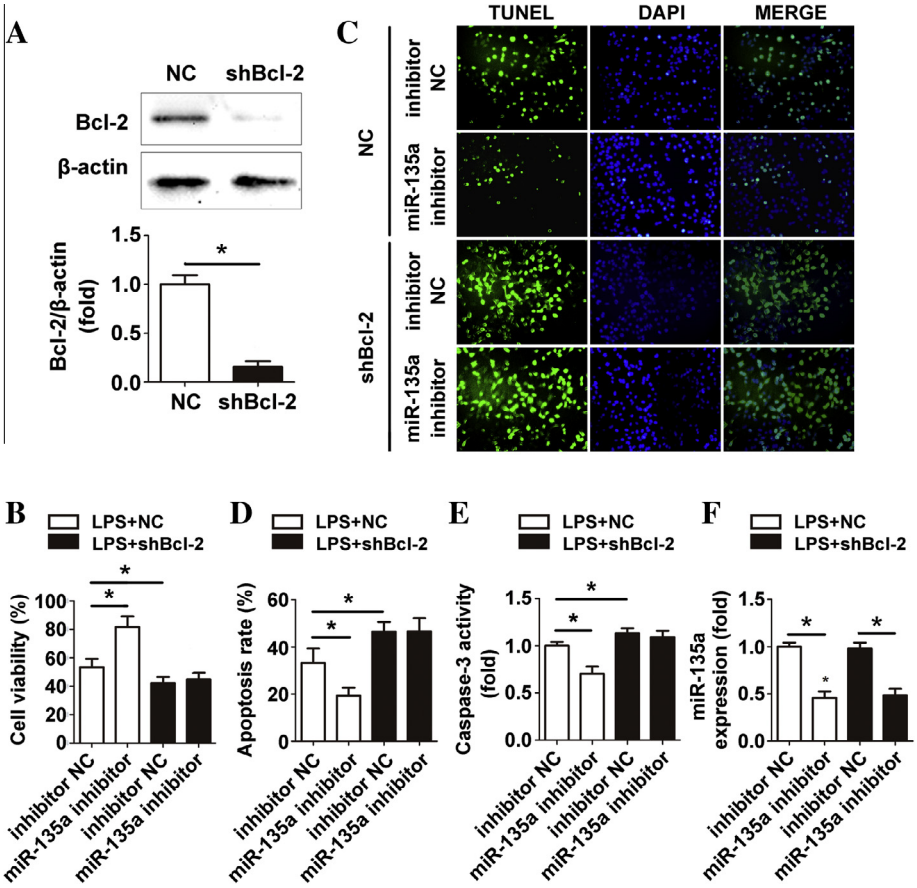

Fig. 4. miR-135a regulates LPS-induced apoptosis via Bcl-2 modulation. (A) Protein expression of Bcl-2 after knockdown with lentiviral shRNA. β-Actin was used as the internal control ($n = 3$). (B) A549 cell viability ($n = 6$). (C) Apoptosis observed by the TUNEL assay in A549 cells. The fluorescent signals from fragmented DNA (green) and nuclei (blue) were visualized and photographed under an inverted fluorescence microscope (200×). (D) The bar graph represents the quantification of TUNEL-positive cells; positive cells were counted in 10 visual fields. The apoptosis rate was determined as TUNEL-positive cells/DAPI. (E) Caspase-3 activity of A549 cells ($n = 6$). (F) The expression of miR-135a in A549 cells ($n = 6$). NC indicates cells transduced with the negative control; shBcl-2, cells transduced with Lenti-shBcl-2. All data are expressed as the mean ± SD. $^*P < 0.05$. (For interpretation of the references to color in this figure legend, the reader is referred to the web version of this article.)

apoptosis after LPS treatment in comparison to the LPS + inhibitor NC group. More importantly, the level of the anti-apoptosis protein Bcl-2 was significantly increased after miR-135a inhibitor transfection following LPS treatment (Fig. 3E). Taken together, these data suggest that miR-135a inhibition attenuates LPS-induced apoptosis in A549 cells; this protective effect may be attributed to Bcl-2 upregulation mediated by miR-135a inhibition.

To further investigate the relevance of miR-135a/Bcl-2 signaling in this model, we knocked down Bcl-2 expression in A549 cells with a lentivirus-based Bcl-2 shRNA. As shown in Fig. 4A, Bcl-2 protein expression was knocked down in cells transduced with shBcl-2, whereas there was no reduction in the cells transfected with the negative control. As expected, in the groups transfected with inhibitor NC (Fig. 4B–E, the first group and the third group), the knockdown of Bcl-2 decreased cell viability and increased the proportion of TUNEL-positive nuclei and caspase-3 activity in LPS-induced apoptosis. In the groups with normal Bcl-2 expression (LPS + NC), miR-135a inhibition showed protective effects similar to those described above (Fig. 4B–E). Interestingly, the miR-135a inhibitor did not protect the A549 cells in which Bcl-2 had been knocked down from LPS-induced apoptosis (LPS + shBcl-2, Fig. 4B–E), despite the downregulation of miR-135a (Fig. 4F).

4. Discussion

In the present study, we have demonstrated that the LPS-induced in vitro model of ALI involves the miR-135a/Bcl-2 signaling pathway. miR-135a was strongly upregulated in A549 cells after LPS treatment, accompanied by the downregulation of Bcl-2. Suppression of miR-135a by a specific inhibitor directly enhanced the expression of Bcl-2 and ameliorated the induction of apoptosis by LPS. Furthermore, we knocked down the expression of Bcl-2 in A549 cells under LPS-treated conditions. Interestingly, we found that inhibition of miR-135a did not attenuate apoptosis in cells with Bcl-2 knockdown, demonstrating that miR-135a regulates apoptosis at least partly through the regulation of Bcl-2. To the best of our knowledge, this is the first study examining the role of miRNAs in mediating apoptosis via Bcl-2 in an LPS-induced in vitro ALI model.

Clinical and experimental observations have suggested that apoptosis is a major feature of ALI, and LPS is considered to play a key role in the development of ALI by stimulating apoptosis [5–7]. In this study, significant apoptosis was observed after LPS treatment and was accompanied by caspase-3 activation. These findings were consistent with those of previous studies. During the development of apoptosis, Bcl-2 plays an anti-apoptotic role by controlling the permeabilization of the mitochondrial outer membrane [8]. Previous studies have indicated that Bcl-2 overexpression renders many cell types resistant to diverse apoptotic stimuli [17–19]. Conversely, we and others have demonstrated that Bcl-2-deficient cells are more susceptible to apoptotic induction (Fig. 4B–E) [9,10]. Combined with the suppression of Bcl-2 after LPS treatment, it is conceivable that Bcl-2 is involved in LPS-induced apoptosis.

There are several reports concerning the regulation of Bcl-2 by miRNAs. miR-16 was identified as a regulator of Bcl-2 during the regulation of apoptosis in gliomas [20], and miR-195 and miR-497 were shown to downregulate Bcl-2 in response to tongue squamous cell carcinoma and focal cerebral ischemia, respectively [21,22]. These observations suggest that the regulation of Bcl-2 may be controlled by miRNAs during LPS-induced apoptosis. To address this possibility, a bioinformatic analysis was conducted to screen for miRNAs targeting Bcl-2. Next, aberrant expression levels of these miRNAs were assessed in A549 cells after LPS treatment. Among the miRNAs with expression levels that were significantly altered, miR-135a was dramatically increased, by 5.01-fold. An increasing number of reports have indicated that the miRNAs that are found to change most dramatically may play critical roles in various pathophysiological processes [14,15,21]. Indeed, we found that miR-135a inhibition remarkably restored Bcl-2 expression and protected A549 cells from LPS-induced apoptosis. Taken together, we suggest that miR-135a is a potential regulator of LPS-induced apoptosis. Moreover, the protective effects of miR-135a inhibition may be attributable to the regulation of Bcl-2.

Recent data have suggested that miRNAs exert important post-transcriptional regulatory functions. miRNAs bind to complementary sites on target mRNA sequences and induce the cleavage of the transcript or block translation [13]. Our results show that miR-135a overexpression decreased the levels of Bcl-2 protein. Conversely, the inhibition of miR-135a increased Bcl-2 levels. Interestingly, Bcl-2 mRNA levels did not change in response to a miR-135a mimic or inhibitor, indicating that miR-135a regulates Bcl-2 expression by repressing translation rather than through mRNA degradation. To further study the mechanisms of miR-135a as a novel regulator of Bcl-2 protein expression in this model, luciferase activity assays were performed. Bcl-2 3′-UTR luciferase activity was significantly repressed with miR-135a overexpression, but this repression was not observed with mutated Bcl-2-3′-UTR. These data confirm that the miR-135a binding site in the Bcl-2 3′-UTR mediated this repression. Taken together, we suggest that Bcl-2 expression is directly regulated by miR-135a in this model.

miR-135a has been shown to regulate many target genes and thus influence a variety of physiological and pathological processes. For example, bone morphogenetic protein receptor and JAK2 are both directly regulated by miR-135a and play important roles in tooth formation and hodgkin lymphoma cells apoptosis, respectively [23,24]. These facts prompted us to determine whether the regulation of Bcl-2, another important target gene of miR-135a, plays a critical role in the development of LPS-induced apoptosis. To test this, we knocked down Bcl-2, and our data showed that Bcl-2 knockdown decreased cell viability and increased apoptosis. Interestingly, a miR-135a inhibitor did not increase cell viability or ameliorate apoptosis in the cells with Bcl-2 knockdown, despite a marked downregulation of miR-135a. Therefore, it is plausible that miR-135a regulates LPS-induced A549 apoptosis via the modulation of Bcl-2.

A recent report revealed that a set of miRNAs (miR-16, miR-17, miR-20a, miR-20b and miR-26a) showed significant alterations in the serum from septic mice [25]; however, those changes were different from our results for in vitro sepsis-induced ALI. These data suggest that the regulation of miRNAs may differ between serum and the lung. Moreover, although miR-135a was significantly elevated in A549 cells after LPS treatment, a variety of miRNAs were altered simultaneously. These miRNAs may have synergistic effects in the regulation of apoptosis. Furthermore, the in vitro sepsis-induced ALI model can only partly reflect the in vivo pathophysiology, which may be a limitation of the current study. To explore the details of this mechanism in vivo, we are currently performing separate and more extensive experiments including locked-nucleic acid-mediated miR-135a suppression in the lungs of septic mice.

In summary, our results demonstrate a mechanism for miR-135a in regulating LPS-induced apoptosis in A549 cells via the targeting of Bcl-2. These findings may represent a novel therapeutic avenue for ALI induced by LPS or sepsis.

Acknowledgment

This work was supported by grants from the Chinese National Natural Science Foundation (No. 30870699).

References

[1] P.E. Parsons, M.A. Matthay, L.B. Ware, M.D. Eisner, Elevated plasma levels of soluble TNF receptors are associated with morbidity and mortality in patients with acute lung injury, Am. J. Physiol. Lung Cell Mol. Physiol. 288 (2005) L426–L431.
[2] L.D. Hudson, J.A. Milberg, D. Anardi, R.J. Maunder, Clinical risks for development of the acute respiratory distress syndrome, Am. J. Respir. Crit. Care Med. 151 (1995) 293–301.
[3] E. Roupie, E. Lepage, M. Wysocki, J.Y. Fagon, J. Chastre, D. Dreyfuss, H. Mentec, J. Carlet, C. Brun-Buisson, F. Lemaire, L. Brochard, Prevalence, etiologies and outcome of the acute respiratory distress syndrome among hypoxemic ventilated patients. SRLF Collaborative Group on Mechanical Ventilation. Societe de Reanimation de Langue Francaise, Intensive Care Med. 25 (1999) 920–929.
[4] L.B. Ware, M.A. Matthay, The acute respiratory distress syndrome, N. Engl. J. Med. 342 (2000) 1334–1349.
[5] M. Rojas, C.R. Woods, A.L. Mora, J. Xu, K.L. Brigham, Endotoxin-induced lung injury in mice: structural, functional, and biochemical responses, Am. J. Physiol. Lung Cell Mol. Physiol. 288 (2005) L333–L341.
[6] R.M. Sweeney, M. Griffiths, D. McAuley, Treatment of acute lung injury: current and emerging pharmacological therapies, Semin. Respir. Crit. Care Med. 34 (2013) 487–498.
[7] M.P. Messer, P. Kellermann, S.J. Weber, C. Hohmann, S. Denk, B. Klohs, A. Schultze, S. Braumuller, M.S. Huber-Lang, M. Perl, Silencing of fas, fas-associated via death domain, or caspase 3 differentially affects lung inflammation, apoptosis, and development of trauma-induced septic acute lung injury, Shock 39 (2013) 19–27.
[8] J.J. Steinle, Retinal endothelial cell apoptosis, Apoptosis 17 (2012) 1258–1260.
[9] L.A. Martin, M. Dowsett, BCL-2: a new therapeutic target in estrogen receptor-positive breast cancer?, Cancer Cell 24 (2013) 7–9
[10] A. Stefanikova, K. Klikova, J. Hatok, P. Racay, ABT-737 accelerates butyrate-induced death of HL-60 cells. Involvement of mitochondrial apoptosis pathway, Gen. Physiol. Biophys. 32 (2013) 505–516.
[11] L. Li, W. Wu, W. Huang, G. Hu, W. Yuan, W. Li, NF-kappaB RNAi decreases the Bax/Bcl-2 ratio and inhibits TNF-alpha-induced apoptosis in human alveolar epithelial cells, Inflamm. Res. 62 (2013) 387–397.
[12] C. Feng, L. Zhang, C. Nguyen, S.N. Vogel, S.E. Goldblum, W.C. Blackwelder, A.S. Cross, Neuraminidase reprograms lung tissue and potentiates lipopolysaccharide-induced acute lung injury in mice, J. Immunol. 191 (2013) 4828–4837.
[13] K.U. Tufekci, R.L. Meuwissen, S. Genc, The role of microRNAs in biological processes, Methods Mol. Biol. 1107 (2014) 15–31.
[14] X.F. Ke, J. Fang, X.N. Wu, C.H. Yu, MicroRNA-203 accelerates apoptosis in LPS-stimulated alveolar epithelial cells by targeting PIK3CA, Biochem. Biophys. Res. Commun. 450 (2014) 1297–1303.
[15] B. Zhang, M. Zhou, C. Li, J. Zhou, H. Li, D. Zhu, Z. Wang, A. Chen, Q. Zhao, MicroRNA-92a inhibition attenuates hypoxia/reoxygenation-induced myocardiocyte apoptosis by targeting Smad7, PLoS One 9 (2014) e100298.
[16] C.Y. Chuang, T.L. Chen, Y.G. Cherng, Y.T. Tai, T.G. Chen, R.M. Chen, Lipopolysaccharide induces apoptotic insults to human alveolar epithelial A549 cells through reactive oxygen species-mediated activation of an intrinsic mitochondrion-dependent pathway, Arch. Toxicol. 85 (2011) 209–218.
[17] A. Luna-Lopez, V.Y. Gonzalez-Puertos, J. Romero-Ontiveros, J.L. Ventura-Gallegos, A. Zentella, L.E. Gomez-Quiroz, M. Konigsberg, A noncanonical NF-kappaB pathway through the p50 subunit regulates Bcl-2 overexpression during an oxidative-conditioning hormesis response, Free Radic. Biol. Med. 63 (2013) 41–50.
[18] C.Z. Kong, Z. Zhang, Bcl-2 overexpression inhibits generation of intracellular reactive oxygen species and blocks adriamycin-induced apoptosis in bladder cancer cells, Asian Pac. J. Cancer Prev. 14 (2013) 895–901.
[19] H. Zhang, Q. Li, Z. Li, Y. Mei, Y. Guo, The protection of Bcl-2 overexpression on rat cortical neuronal injury caused by analogous ischemia/reperfusion in vitro, Neurosci. Res. 62 (2008) 140–146.
[20] T.Q. Yang, X.J. Lu, T.F. Wu, D.D. Ding, Z.H. Zhao, G.L. Chen, X.S. Xie, B. Li, Y.X. Wei, L.C. Guo, Y. Zhang, Y.L. Huang, Y.X. Zhou, Z.W. Du, MicroRNA-16 inhibits glioma cell growth and invasion through suppression of BCL2 and the nuclear factor-kappaB1/MMP9 signaling pathway, Cancer Sci. 105 (2014) 265–271.

[21] K.J. Yin, Z. Deng, H. Huang, M. Hamblin, C. Xie, J. Zhang, Y.E. Chen, MiR-497 regulates neuronal death in mouse brain after transient focal cerebral ischemia, Neurobiol. Dis. 38 (2010) 17–26.
[22] L.F. Jia, S.B. Wei, K. Gong, Y.H. Gan, G.Y. Yu, Prognostic implications of microRNA miR-195 expression in human tongue squamous cell carcinoma, PLoS One 8 (2013) e56634.
[23] E.J. Kim, M.J. Lee, L. Li, K.S. Yoon, K.S. Kim, H.S. Jung, Failure of tooth formation mediated by miR-135a overexpression via BMP signaling, J. Dent. Res. 93 (2014) 571–575.
[24] A. Navarro, T. Diaz, A. Martinez, A. Gaya, A. Pons, B. Gel, C. Codony, G. Ferrer, C. Martinez, E. Montserrat, M. Monzo, Regulation of JAK2 by miR-135a: prognostic impact in classic Hodgkin lymphoma, Blood 114 (2009) 2945–2951.
[25] S.C. Wu, J.C. Yang, C.S. Rau, Y.C. Chen, T.H. Lu, M.W. Lin, S.L. Tzeng, Y.C. Wu, C.J. Wu, C.H. Hsieh, Profiling circulating microRNA expression in experimental sepsis using cecal ligation and puncture, PLoS One 8 (2013) e77936.